Functional comparison of protein domains within aPKCs involved in nucleocytoplasmic shuttling

Sebastian Seidl, Ursula B. Braun and Michael Leitges*

Biotechnology Centre of Oslo, University of Oslo, NO-0349, Oslo, Norway

*Author for correspondence (michael.leitges@biotek.uio.no)

Biology Open 1, 436–445
doi: 10.1242/bio.2012505

Summary

The atypical protein kinases C (PKC) isoforms ι and ζ play crucial roles in regulation of signaling pathways related to proliferation, differentiation and cell survival. Over the years several interaction partners and phosphorylation targets have been identified. However, little is known about the regulation of atypical aPKC isoforms. To address this question, we performed a comparative analysis of atypical aPKCι/λ and ζ in MDCK cells. By using green fluorescence protein (GFP) fusion proteins containing the full-length or truncated proteins, we were able to recognize differences in subcellular localization and nucleocytoplasmic shuttling of both isoforms. We show, that an earlier described nuclear localization sequence (NLS), plays a role in the regulation of atypical aPKCζ but not in aPKCι, despite the fact that it is present in both isoforms. Leptomycin B treatment induces accumulation of GFP-fusion protein of both isoforms in the nucleus. Regardless, the loss of the NLS only decreases shuttling of aPKCζ, while aPKCι remains unaffected. In addition, we identified the hinge region as a potential regulator of localization of atypical PKCs. With a set of chimeric proteins we show that the hinge region of aPKCι mediates nuclear localization. In contrast, the hinge region of aPKCζ causes exclusion from the nucleus, indicating two different mechanisms leading to isoform specific regulation. Taken together, we show for the first time, that the atypical isoforms aPKCι and ζ underly different mechanisms regarding their regulation of subcellular localization and translocation into the nucleus in MDCK cells.

Key words: GFP-fusion protein, HINGE domain, NLS, Atypical Protein kinase C, Nuclear translocation, Nucleocytoplasmic shuttling

Introduction

Signal transduction is an essential process that enables the cell to interpret incoming signals and interact with the surrounding environment. Many different signaling pathways and a wide variety of mechanisms are utilized to accomplish this translation. Kinase activation is a very common mechanism that alone can amplify the incoming signal through the phosphorylation of specific substrates. Kinase substrates are often themselves kinases.

Protein Kinase C (PKC) represents a serine/threonine kinase gene family that has often been described as having a major role in signal transduction events. Nine PKC members have been described in mammals which are divided into three subgroups based on their biochemical properties and sequence homology: Classical PKCs (α, β and γ), novel PKCs (δ, ε, θ and *η*) and atypical PKCs (ζ and ι/λ). Classical and novel PKCs have been found to bind and be activated by tumor-promoting phorbol esters (TPA) which has connected at least some of their physiological in vivo functions to the promotion of cancer.

Atypical PKCs were the last to be identified and characterized. Remarkably, early findings showed that both aPKC isoforms are unresponsive to TPA and are also activated independently of calcium and diacylglycerin under normal cell conditions. Thus aPKCs represent a PKC subgroup that is clearly separated from the rest by its mode of activation. Both atypical PKC isoforms have been found to be regulated through their cysteine-rich C1 domain by Par-4 activation (Díaz-Meco et al., 1996) and through their Phox/Bem1 (PB1) domain by interaction with p62 and PAR-6 (Puls et al., 1997; Joberty et al., 2000; Sánchez et al., 1998). Another striking point within the aPKC subgroup is the high content of homologous amino acids between them (72% overall) (Akimoto et al., 1994) which limits the availability of isoform-specific tools. Thus it remains difficult to biochemically analyze and distinguish between the two aPKC isoforms. In addition, many overexpression studies have so far failed to assign functional differences to PKCζ and PKCι/λ (Diaz-Meco and Moscat, 2001; Uberall et al., 1999).

Nevertheless recent attempts utilizing the gene targeting approach in mice have revealed that highly specific in vivo functions exist for both aPKCs. For example, the phenotypical analysis of the PKCζ deficient mouse line lead to the identification of impairment of the NFkB signalling pathway (Leitges et al., 2001) as well as changes in IL-4 and IL-6 signaling (Martin et al., 2002; Galvez et al., 2009). A conventional knock-out of PKCι/λ revealed a fundamental role for this kinase during embryonic development (Bandyopadhyay et al., 2004; Soloff et al., 2004; unpublished data). Tissue specific knockouts of this isoform have also shown the importance of PKC ι/λ in the adult organism (Farese et al., 2007; Huber et al., 2009; Murray et al., 2009; Yang et al., 2009).

Whereas the embryonic lethal phenotype of PKCι/λ could be partly explained by the lack of PKCζ expression at the defined

time of development (Kovac et al., 2007) all other described phenotypes of both aPKC knockouts take place with the existence of the alternate aPKC isoform. Thus these in vivo findings clearly imply that both aPKCs have an isoform-specific, non-redundant function in the cell, even when co-expressed. How these specificities are regulated remains largely unclear. Since specific localization of PKCs within a cell is believed to be one way of controlling specificity (Rosse et al., 2010) we decided to screen for domains within both aPKCs which are able to direct localization and are different between the two isoforms.

Results

1. Generation of truncated aPKC/GFP fusion proteins.

We have used truncated aPKC proteins fused with a GFP tag to follow and identify domains that confer aPKC isoform specific translocation ability. Except for the full length constructs of both isoforms, we have generated mutant constructs that focus on changes in the N-terminal regulatory region of the proteins and have a truncated C-terminal, thus they are missing the kinase domain. Although we cannot say that translocation sequences do not exist in the C-terminal kinase region, we expected to see more changes in translocation potential upon alteration of the N-terminal regulatory region. Thus we initially generated the following for both isoforms: the GFP labeled full length construct; an (aPKC$^{\Delta catalytic}$) construct missing the whole kinase domain including a nuclear export sequence (NES); an N-terminal version (aPKC AA1-176(177*)) including the PB1 (Phox and Bem1) and a C1 (cystein-rich) domain but excluding the hinge region. We further generated a construct consisting of the hinge region alone (aPKC^{HINGE}) (Fig. 1A). All fusion proteins have been tested for expression and stability of the protein in MDCK cells via western blot (supplementary material Fig. S1).

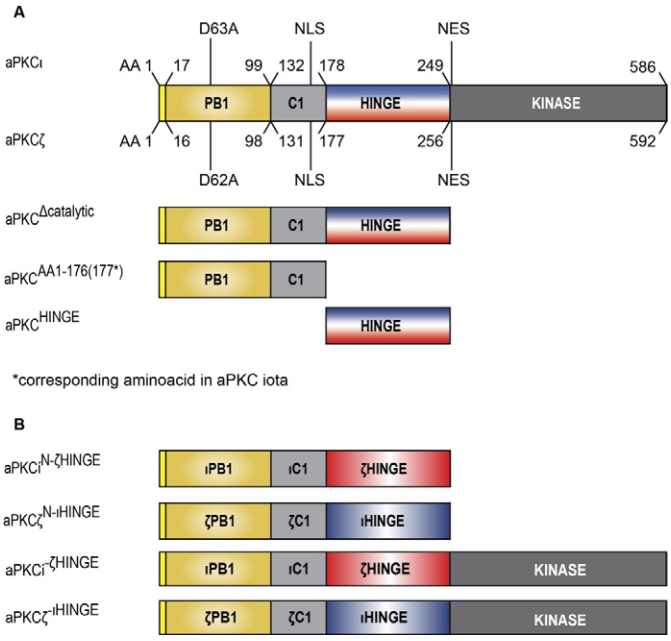

Fig. 1. Schematic presentation of GFP-fusion proteins. Domain organization of atypical PKC and the constructs generated to test the localization of truncated atypical PKC proteins. All proteins were expressed as a GFP fusion protein with a C-terminal tag.

2. Isoform-specific domains cause different subcellular localization.

To test whether the truncation mutants are able to identify domains within aPKCs which convey isoform-specific localization we overexpressed each construct in MDCK cells. Both full length constructs showed a widely distributed diffuse GFP signal over the whole cell without prominent membrane localization. There was a slightly increased PKCι nuclear localization when compared to aPKCζ full length (Fig. 2A,B).

Deletion of the C-terminal kinase domain changed the distribution. The aPKCι$^{\Delta catalytic}$ fusion protein localized exclusively in the nucleus with a regional concentration of the GFP signal within the nucleolus (Fig. 2C). In sharp contrast the corresponding truncated PKCζ$^{\Delta catalytic}$ construct showed an almost exclusive and very strong membrane signal (Fig. 2D) which resembled that associated with the role of aPKC in polarity.

We proceeded by testing N-terminal truncations missing the hinge region (aPKC$^{AA1-176(177)}$) and found there was a reversion back to a similar localization pattern between the two isoforms (Fig. 2E,F). However, in contrast to the full length proteins, both truncated versions located to the nucleus with a distinct punctate pattern. This pattern was different to that seen with the aPKCι$^{\Delta catalytic}$ form.

Based on these results further investigation focused on the hinge region alone was merited. Analysis of the aPKCι^{HINGE} construct showed a dominant localization to the nucleus as well as a diffuse weak staining in the cytoplasm (Fig. 2G). The corresponding PKCζ^{HINGE} construct showed cytoplasmic staining with some aggregates surrounding the nucleus, no membrane staining, and most significantly, an exclusion from the nucleus (Fig. 2H).

Taken together these results identified first that the hinge region of both aPKCs harbors information important for subcellular localization and second that the N-terminal causes localization to the nucleus and does not need the hinge region for this localization to occur.

3. Functional investigation of aPKC nuclear localization sequence (NLS).

Given the fact that nuclear localization of aPKC represents a new area of research in aPKC in vivo function, we decided to investigate the underlying mechanism. A functional nuclear localization sequence (NLS) located within the C1 domain had been defined in both aPKCs (Perander et al., 2001). To evaluate whether this motif drives the PKCι$^{AA1-177}$ fragment into the nucleus within our experimental context we mutated the amino acid sequence AKRNFRR to AKRNFEE in order to generate a nonfunctional NLS. Upon transfection with this construct in MDCK cells we were not able to detect any difference to that found with the parental construct (data not shown). These findings suggested that the N-terminal PKCι$^{AA1-177}$ fragment translocates into the nucleus in an NLS independent manner through a different mechanism and we assumed that this was also true for the N-terminal PKCζ$^{AA1-176}$ fragment.

We next asked whether the NLS could have an impact on the kinetics of nuclear translocation of both aPKCs. Differences in the nuclear translocation kinetics among aPKCs had been earlier discussed by others (Perander et al., 2001). Based on the finding that N-terminal constructs localize to the nucleus we next worked with full length constructs for both aPKCs in order to analyze the

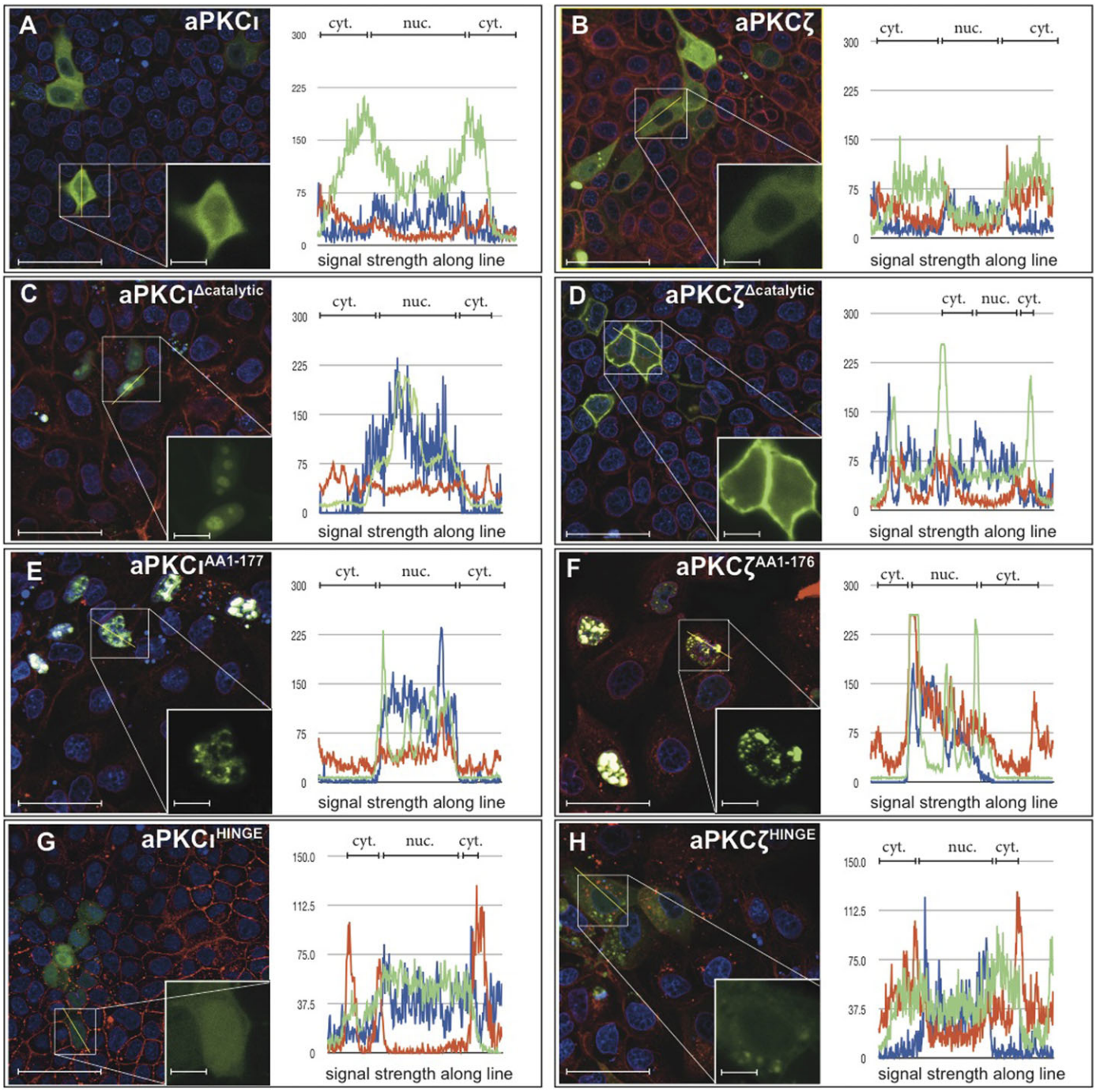

Fig. 2. Differences in sub-cellular localization of truncated aPKC protein. MDCK cells were transfected with different aPKCι **(A,C,E,G)** or aPKCζ fusion proteins **(B,D,F,H)**. The insert shows magnification of the marked area (square) in the overview. Visualization of the nucleus was achieved by DAPI staining. Membrane staining was performed using Alexa Fluor® 647 conjugated wheat-germ agglutinin (WGA). All pictures were taken with the ZEISS LSM 520 microscope. The areas representing the cytosolic fraction or nuclear fraction are indicated with bars at the top of each histogram. The histogram analysis was performed with the 'profile tool' in the LSM Meta® software. The analyzed area is indicated by the yellow straight line in the overview. Scale bar: 50 µm (overview), 10 µm (insert). All experiments were performed in triplicates.

translocation kinetics upon Leptomycin B (LMB) treatment. Treatment with LMB effectively blocks all nuclear export related to CRM1/Exportin and represents an established method to study nucleo-cytoplasmic shuttling (Lischka et al., 2001; Kudo et al., 1998).

When comparing mouse aPKC cDNA sequences we observed that aPKCζ contains a G to R exchange at position 141(AKRFNRG; supplementary material Fig. S3). This sequence variation in the NLS had been described to affect the binding of importin α/β and subsequently affect the nuclear translocation

kinetics since the AKRNFRR motif containing three arginine's (as found in PKCι) enables a direct binding of importin β instead of a sequential binding of importin α followed by importin β (Palmeri and Malim, 1999). Thus we first analyzed the translocation behavior of both full length aPKC-GFP fusion constructs by measuring the GFP signal ratio between the cytosol and the nucleus. Both aPKCs accumulated in the nucleus upon LMB treatment but it was clear that PKCι accumulated faster and attained a higher level after 6 hours of treatment (Fig. 3).

We next introduced a construct with an R to G mutation at position 142 in PKCι which mimics a PKCζ NLS. We found that the kinetics of nuclear accumulation upon LMB treatment did not change at all with this construct, which was opposite to our expectations. We then generated a R141/142E mutation in the PKCι/GFP full length construct thereby destroying the NLS motif. The subsequent analysis of this mutant (aPKCι R141/142E) again revealed no significant change in the nuclear translocation behavior of PKCι thus the NLS present in aPKCι appears to be nonfunctional in the context we tested here.

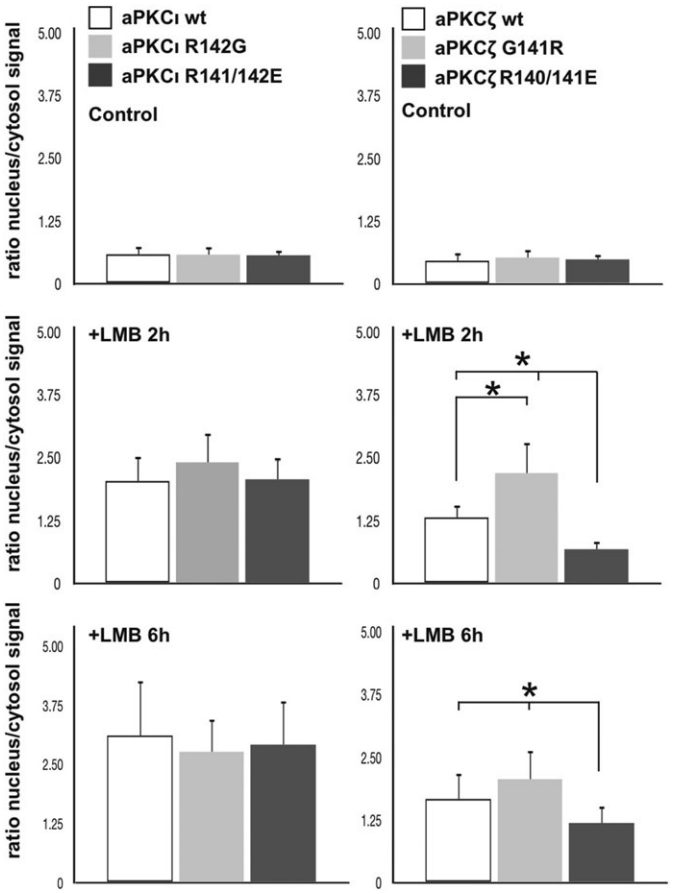

Fig. 3. Nucleocytoplasmic shuttling is dependent on the NLS in the case of aPKC ζ but not aPKC ι. MDCK cells either expressing full-length aPKC wild-type protein of aPKCι (left panel) or aPKCζ (right panel) or the indicated mutation within the NLS of both isoforms. The cells were left untreated in normal medium for 18 hours after transfection with Lipofectamin. Afterwards, the cells were treated with 4 ng/ml Leptomycin B in normal growth medium for either 2 or 6 hours and fixed afterwards with 4% paraformaldehyde. Analysis was done by using the Zeiss LSM 510 confocal microscope. Calculation of ratios between nuclear signal and cytoplasmic signal were performed as described in the methods section. $n=40$, $^*P<0.05$. All experiments were performed in triplicates.

We then concentrated on PKCζ, first generating a mutant of the full length construct which mimics the PKCι situation (aPKCζ G141R). As indicated in Fig. 3, this conversion lead to a faster increase and higher amount of the nuclear signal after 2 hours with no significant change after 6 hours, thus resembling the aPKCι wildtype situation. Next we analyzed the aPKCζ R140E/G141E mutant representing a NLS deficient aPKCζ variant. In this case we were able to detect a significant decrease of the nuclear fraction after 2 and 6 hours LMB treatment implying that the NLS in PKCζ is functionally involved in the nuclear transport of this aPKC. Nevertheless it was also clear that even in the NLS deficient situation a smaller fraction is translocated to the nucleus suggesting that beside the NLS driven transport other nuclear transport mechanism(s) exist which aid in the localization of PKCζ to the nucleus (Fig. 3).

Taken together the mutational analysis of the NLS of both aPKCs revealed that PKCι can translocate to the nucleus independent of its NLS whereas PKCζ's nuclear translocation is mainly regulated by its NLS. In addition we observed that the sequence variant we identified in mouse for PKCζ slows the translocation kinetics and also that PKCζ retains a nuclear translocation capacity that is independent of the NLS.

4. Mutations within the PB1 domain alter the subcellular localization of both aPKCs.

Having established that the generation of a NLS deficient N-terminal PKCι$^{AA1\text{-}177}$ fragment does not abolish its nuclear localization we decided to investigate the possibility of other nuclear translocation domains existing within this fragment. Besides the C1 domain which includes the discussed NLS, another protein-protein interacting domain has been described in the N-terminus of both aPKCs; the Phox/Bem1 (PB1) domain. Several PB1 aPKC interacting proteins have been identified e.g. Par6 and p62 (Joberty et al., 2000; Hirano et al., 2004). Of particular interest in this context is a recent report describing the translocation of Par6 to the nucleus via an internal NLS (Cline and Nelson, 2007). Thus we hypothesized that aPKCs may be translocated to the nucleus through a "hitchhiking" mechanism by their binding to PB1 containing proteins, like Par6. To verify this hypothesis we first introduced a D63A mutation in the PKCι$^{AA1\text{-}177}$ fragment. This D-A mutation has been shown by Hirano to disrupt interaction between the aPKC PB1 domain and the PB1 domain of Par6 and p62 (Hirano et al., 2004; Hirano et al., 2005). However, the abolishment of a functional PB1 domain did not prevent a nuclear translocation of this construct (Fig. 4A,B). In addition, the corresponding D62A mutation in the PKCζ$^{AA1\text{-}176}$ fragment reflected the same outcome (Fig. 4C,D). Thus we assumed that in both atypical PKC N-terminal fragments either a cryptic NLS or another sequence motif existed that was responsible for the observed nuclear localization.

We then focused attention on the analysis of the full length protein fusions to investigate the consequence of a PB1 mutation in aPKC nuclear localization in this context. Thus we introduced the D63A or D62A mutations respectively in each full length aPKC construct which we subsequently analyzed in an LMB experiment.

In order to verify the functionality of the introduced mutation we first checked whether the PB1 mutation caused a loss of membrane association due to the protein's inability to form the polarity complex with Par6/aPKC/Par3 (Lin et al., 2000; Wodarz

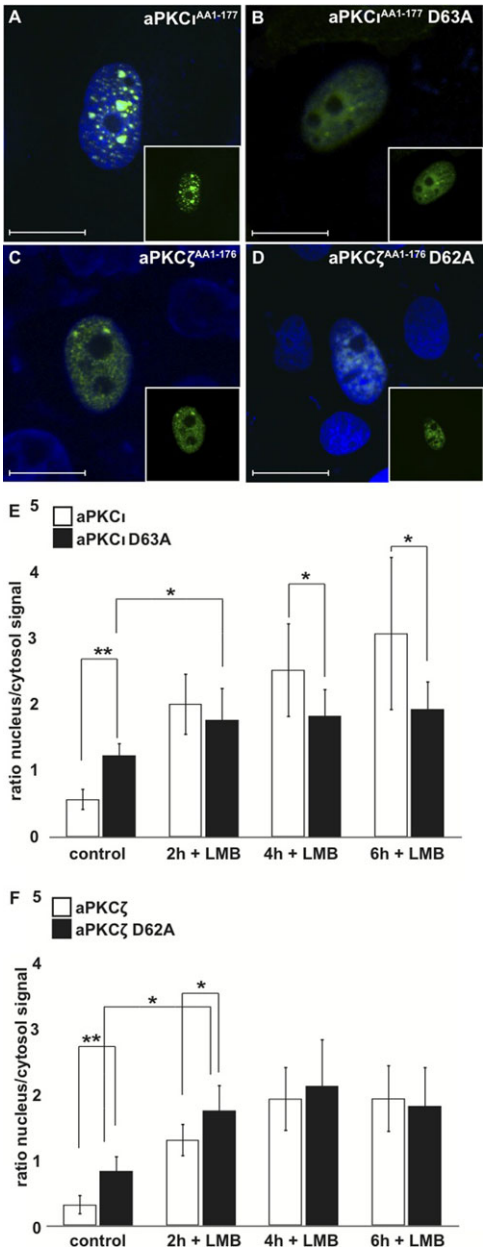

Fig. 4. The PB1 domain of atypical PKCs influences localization of both atypical isoforms. MDCK cells were either transfected with a construct expressing the regulatory domain of aPKCι **(A)** or aPKCζ **(C)** wildtype, or corresponding mutant proteins **(B,D)**. Cells were tranfected with Lipofectamin© and left untreated for 18 hours before preparation for imaging analysis. Visualization of the nucleus was achieved by DAPI staining. Analysis was done by using the Zeiss LSM 510 confocal microscope. Scale bar: 10 μm. **(E,F)** MDCK cells either expressing full-length aPKC wild-type protein or full-length protein containing a PB1 mutation of aPKCι (E) or aPKCζ (F). Eighteen hours after transfection cells were treated with 4 ng/ml leptomycin B in normal growth medium for 2, 4 and 6 hours before preparation for imaging analysis. Calculation of ratios between nuclear signal and cytoplasmic signal were performed as described in the methods section. $n=40$, $*P<0.05$. All experiments were performed in triplicates.

et al., 2000; Joberty et al., 2000). In fact, we observed a clear decrease of GFP membrane signal in both constructs, indicating the introduced mutation was functionally significant (supplementary material Fig. S2). Upon further analysis of the subcellular localization of these constructs we observed that both aPKC isoforms harboring the D to A mutation showed a significant increase in the pool of nuclear located fusion protein in the non-LMB treated samples (Fig. 4E,F, control values).

With regard to PKCζ, LMB treatment caused a similar kinetic rate of nuclear accumulation for both wild type and mutated constructs whereby the D62A mutant translocation started at a significantly higher level, but both reached maximum accumulation levels after 4 hours of LMB treatment (Fig. 4F).

In contrast, PKCι gave a different picture of nuclear accumulation. Whereas the wild type construct increased its amount in the nucleus constantly over the 6 hour time line, the D63A mutation of PKCι increased its nuclear level only slightly (but significantly) within the first 2 hours. We were unable to detect any further significant increase of the mutant construct in the nucleus beyond this time-point (Fig. 4E).

Taken together we have shown that the PB1 domain within both aPKCs is not involved in the nuclear translocation of the N-terminal constructs used here indicating the existence of an alternate nuclear translocation mechanism for these two fusion proteins. However, this analysis also revealed that in the context of the full length protein, the PB1 domain does influence the localization of aPKCs in an isoform specific manner: whereas PKCζ appears to translocate into the nucleus independent of its PB1 domain, PKCι translocation seemed unable to proceed beyond a certain level of nuclear content (reached at 2 hours after addition of LMB) implying that at least a fraction of the transported GFP fusion protein depends on a functional PB1 domain.

5. Atypical PKCs hinge region mediates different localization of aPKCι and aPKCζ.

Our initial screen revealed that the hinge region of both aPKCs appeared to be involved in the unique sub-cellular localization of each isoform (Fig. 2). To further elucidate these findings we generated mutants with exchanged hinge regions that either harbored the aPKCι specific hinge sequence within the aPKCζ specific background or vice versa (Fig. 1B). Upon transfection of the N-terminal chimeric aPKCι$^{N\text{-}\zeta HINGE}$/GFP fusion protein into MDCK cells it became apparent that the aPKCζ specific hinge sequence is able to keep the aPKCι protein outside of the nucleus (Fig. 5A,C). Interestingly this chimeric fusion protein did not reflect the same pattern as the aPKCζ$^{\Delta catalytic}$ with regard to membrane staining (compare Fig. 5B and Fig. 5C), thus an interplay between the remaining ζ-N-terminus and its hinge region must exist which has the capacity to drive the aPKCζ construct to the membrane.

The corresponding experiment with a aPKCζ$^{N\text{-}\iota HINGE}$/GFP fusion protein showed an exact phenocopy of the parental ι-hinge construct i.e. an exclusive nuclear localization with an enrichment of the GFP signal within the nucleoli (Fig. 5A,B,D).

These findings clearly identified that the hinge region of atypical PKCs can be distinguished as harboring specific sub-cellular localization information.

We then proceeded to ask the same question in the context of the full length protein. We used either wildtype or chimeric fusion proteins which contained the corresponding hinge region of the alternate aPKC isoform (Fig. 1B). We first analyzed the subcellular localization of these constructs by measuring the nuclear to cytosol ratio of the GFP signal. As indicated in Fig. 5E

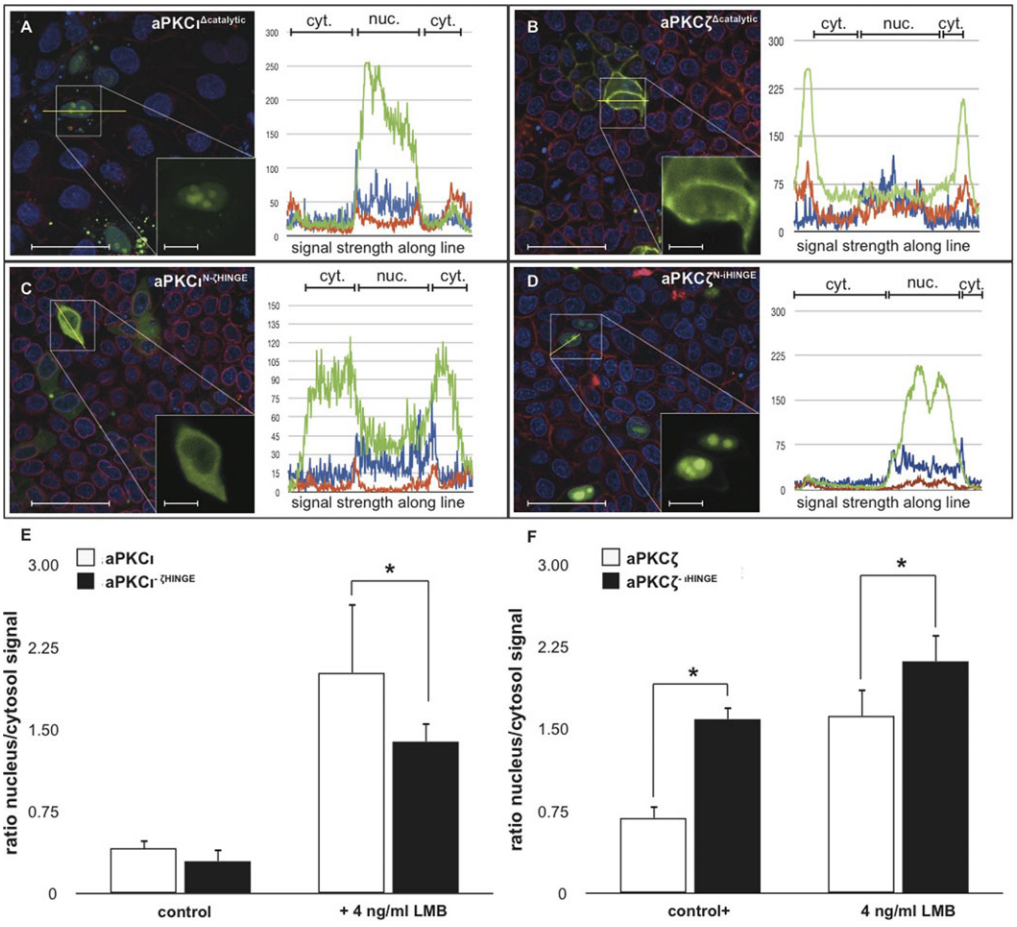

Fig. 5. Atypical PKC hinge region mediates different localization of aPKCι and aPKCζ. MDCK cells were transfected with constructs expressing either the regulatory domain of aPKCι or aPKCζ **(A,B)** or chimeric proteins consisting of the regulatory domain of aPKCι with a aPKCζ hinge region, or vice versa **(C,D)**. The insert shows magnification of the marked area (square) in the overview. Visualization of the nucleus was achieved by DAPI staining. Membrane staining was performed using Alexa Fluor® 647 conjugated wheat-germ agglutinin (WGA). All pictures were taken with the ZEISS LSM 510 microscope. The areas representing the cytosolic fraction or nuclear fraction are indicated with bars at the top of each histogram. The histogram analysis was performed with the 'profile tool' in the LSM Meta® software. The analyzed area is indicated by the yellow straight line in the overview. Scale bar: 50 µm (overview), 10 µm (insert). All experiments were performed in triplicates.

(control lane) an aPKCζ protein harboring a ι-hinge region showed a significant increase in the nuclear fraction of the GFP signal whereas the chimeric aPKCι protein did not appear to be affected by the ζ-hinge region with regard to its nuclear localization (Fig. 5F, control lane). After 6 hours of LMB treatment the chimeric aPKCζ$^{\iota HINGE}$ construct showed a higher accumulation of the GFP signal in the nucleus (at a similar level to that of the aPKCι wildtype construct) (Fig. 5E). In contrast, the chimeric aPKCι$^{\zeta HINGE}$ protein showed a significant decrease of its nuclear signal after 6 hours of LMB treatment thus mimicking the levels reached by the aPKCζ wild type construct (Fig. 5F).

In summary, both approaches identify the hinge region of both aPKCs as a domain that contains isoform specific sub-cellular localization information.

Discussion

Atypical PKCs represent a subgroup of the PKC family distinguished by their mode of activation and their remarkably high homology content to each other (Steinberg, 2008). Most published work on aPKCs has not distinguished between the two isoforms due to the lack of specificity of available tools such as reliably specific antibodies and peptide inhibitors. In addition, due to the high homology of the amino acid sequence, there is a great potential for redundancy between these two isoforms.

Nevertheless studies using either RNA knockdown (Durgan et al., 2011) or gene targeting approaches in mice (Leitges et al., 2001; Farese et al., 2007) clearly indicate the existence of isoform-specific functions. Phenotypical analysis has revealed quite opposite in vivo functions even in cells where both isoforms coexist, for example in the intestinal epithelial cell, (Oster and Leitges, 2006; Murray et al., 2009). Thus the question of how these different functions are regulated given the high degree of homology becomes poignant.

The intention of this study was to identify how specific domains within both isoforms transfer specificity to the individual protein. As described for other PKCs (Parker and Murray-Rust, 2004) we assumed that one method to achieve specificity is through protein localization within the cell. Thus in an unbiased approach we tested aPKC/GFP fusion constructs for their location after their transient transfection in MDCK cells.

In accordance with others (Horikoshi et al., 2009), we found both full length constructs mainly located in the cytoplasm but we also observed that while the aPKCζ construct was excluded from the nucleus the aPKCι construct showed weak nuclear staining implying a tendency for its nuclear localization compared to aPKCζ .

A clear difference between the two isoforms became obvious when analyzing the N-terminal constructs missing the catalytic kinase domain (aPKCζ$^{\Delta catalytic}$ and aPKCι$^{\Delta catalytic}$). It is worth stating here that this truncation eliminates a nuclear export sequence (NES) from both constructs (aPKCζ AA 247–255, aPKCι AA 239–247) and leaves the truncated protein in a somewhat open conformation. Whereas the aPKCζ specific construct showed prominent membrane staining, aPKCι was found exclusively in the nucleus. These observations per se

indicate a clear difference between both aPKC isoforms. The robust membrane localization of aPKCζ could be explained by its previously reported association with the signaling cascade of the ternary polarity par3/aPKC/par6 complex which is localized at the cell membrane (Suzuki et al., 2001), while the accumulation of the aPKCι construct might be a consequence of the missing NES. The explanation for this obvious difference in localization remains elusive.

Further investigation identified the hinge region of both isoforms to be essential in this localization process. We found that in both isoforms the deletion of the hinge domain caused a nuclear localization that was different in appearance to that observed in aPKCι$^{\Delta catalytic}$ construct expression where the hinge region is intact. We also found that expression of hinge/GFP fusion proteins showed an isoform-specific difference.

Whereas the aPKCι^{HINGE} predominantly localized in the nucleus (showing a homogenous distribution within) the aPKCζ^{HINGE} was excluded. Thus, given the fact that the hinge region within aPKCs contains the most diverse nucleotide sequence it is interesting to observe that both isoforms contain information related to isoform-specific, distinct, subcellular localization in this region. This was finally confirmed by the expression of chimeric proteins that were generated containing the hinge fragment of one isoform sub-cloned to the corresponding N-terminus (or full length) of the alternate aPKC isoform (Fig. 5). In both cases ι-hinge drives the protein into the nucleus whereas ζ-hinge either keeps it outside (N-terminal construct) or significantly reduces (in the context of the full length protein) the nuclear pool upon LMB treatment.

Until now, the only verified functional motif within the atypical hinge sequence had been a caspase cleavage site which exists only in aPKCζ and is involved in the regulation of the protein's enzymatic activity rather then its localization (Frutos et al., 1999). Any other functional derivation based on the crude amino acid sequence is highly speculative without experimental verification. Current approaches in our laboratory employed mutagenesis to establish hinge region mutants with abolished localization behavior, thereby enabling the identification of the underlying sequence motifs (and mechanisms) that cause these observed differences between hinge regions in different aPKC isoforms.

The N-terminal construct (depleted of the hinge region) of both aPKCs was found exclusively in the nucleus which could be explained by the NLS motif located in the C1 domain, functionally described by others (Perander et al., 2001; Pu et al., 2006). Nevertheless we investigated the NLS in more detail and showed that mutations destroying the functionality of the NLS did not completely abolish the nuclear translocation of either the N-terminal or the full length GFP fusion proteins in either aPKC. This was a surprising result since the NLS had been shown to cause localization to the nucleus in the context of both a smaller fragment and a full length construct containing a kinase defective mutation in a different cellular context (Perander et al., 2001). We found that neither an N-terminal nor a full length aPKCι/GFP construct containing an R141/142 mutation appeared to be affected in its nuclear translocation behavior. However, a full-length aPKCζ/GFP construct harboring an R140/141 mutation showed a significant reduction in the amount of nuclear accumulation after 2 and 6 hours LMB treatment. Although reduced, the accumulation was significant, thus indicating the possible existence of alternate methods of translocation.

During our analysis we identified a sequence variant in the NLS sequence which appears to be mouse specific and converts the PKCζ specific NLS to AKRFNRG (Uniprot.org entry Q02956). This variation could explain the slower nuclear translocation of PKCζ observed upon LMB treatment compared with PKCι based on the described mechanism of the importin α/β system. Also the G141R mutation of PKCζ which converts the ζ-NLS into a ι-NLS, supports this notion since the construct mimicked the PKCι nuclear translocation kinetics exactly (higher maximum, reached after 2 hours LMB treatment). However, this is not a valid argument for the observed differences regarding the nuclear translocation kinetics between both aPKC isoforms made previously by others (Perander et al., 2001) since the aPKC cDNAs from other species that do not contain this sequence variation were used. Thus, our observation may be either a cell type or species specific phenomena or a combination of both. In any case our data show a clear difference between both aPKCs and their NLS dependent nuclear translocation in MDCK cells upon LMB treatment when using mouse specific constructs. PKCι translocates to the nucleus independently of its NLS whereas PKCζ mainly depends on a functional NLS.

One reason for the NLS independent translocation of PKCι might be hidden in its hinge region which we have shown to be able to direct nuclear translocation. Other mechanisms must also exist since N-terminal constructs of both aPKC isoforms (missing each hinge region and containing NLS mutations) retain the capacity to translocate to the nucleus.

We have further analyzed the PB1 domain which remained intact in our N-terminal constructs and which has been implicated as a mediator of protein-protein interactions between PB1 containing proteins (Hirano et al., 2004; Hirano et al., 2005). To our knowledge, the PB1 interacting proteins include at least 13 mammalian proteins (Lamark et al., 2003).

The background notion for this attempt was that it was possible that interacting partners of aPKCs were able to translocate to the nucleus and could serve as a shuttle vehicle for aPKCs. However, when introducing a D-A mutation which had been described to abolish PB1 specific interactions (Hirano et al., 2004) we were not able to detect any effect on the N-terminal constructs with regard on the nuclear/cytoplasm ratio. Upon the introduction of the same mutation into full length proteins we were readily able to detect an increased nuclear fraction in non-treated cells. We interpreted this result as an indication that there is reduced export rather than increased import.

One likely candidate for the export shuttle might be p62. This protein was originally identified as a binding partner for aPKC (Puls et al., 1997; Sánchez et al., 1998) and has received some attention recently based on its involvement in starvation induced autophagy (Pankiv et al., 2010; Wooten et al., 2008; Lamark et al., 2009). More important for us was the identification of p62 in the nuclear compartment (Bjørkøy et al., 2005) and the finding that the shuttling of p62 between cytoplasm and nucleus appears to be a very dynamic process (Pankiv et al., 2010) similar to that we have observed for aPKC. In addition, most recently it has been shown that p62 is involved in the nuclear export of ALFY (autophagy-linked FYVE) proteins through protein-protein interaction (Clausen et al., 2010). Thus, it could well be that p62 is also involved in the nuclear export of aPKC. Nevertheless, we do not exclude other PB1 containing proteins, like Par6, also

recently described as a nuclear protein (Cline and Nelson, 2007), being involved in the nuclear translocation of aPKC.

With regard to nuclear import, the PB1 mutation did not influence PKCζ (similar kinetics and amounts of nuclear accumulation were seen) but it did reduce the total amount of PKCι in the nucleus upon LMB treatment. Thus a certain fraction of PKCι translocation to the nucleus depends on an as yet undefined PB1 domain protein-protein interaction.

Our study revealed clear differences between the two aPKC isoforms which have not been analyzed in such a comparative structure to function study before. The hinge region, representing the most heterologous amino acid stretch between the two aPKCs, contains isoform-specific, sub-cellular localization information. In particular, with regard to the nuclear localization of aPKCs the functionality of the NLS, the PB1 domain and in the case of PKCι the hinge region, are shown to influence the nuclear import to a different degree when both isoforms are compared directly.

We are not the first to show that aPKC is present in the nucleus but our data suggests that there are multiple modes of nuclear transport that differ between aPKC isoforms. This could mean that the physiological conditions in which each aPKC translocates to the nucleus are distinguishable. What exactly drives PKCζ and PKCι into the nucleus is not clear. Our attempts to locate aPKC/GFP proteins to a more precise sub-nuclear domain or to the nucleus during specific cell cycle periods have thus far been unsuccessful (data not shown).

Another option is the activation of aPKC in the context of NFκB signaling leading to a translocation of NFκB to the nucleus. Besides this translocation, specific phosphorylations are required to regulate NFκB specific gene expression. Ser 311 on the RelA subunit has been identified as a PKCζ target (Duran et al., 2003) but where this phosphorylation takes place remains unknown. Thus it could well be that PKCζ must be translocated into the nucleus to phosphorylate RelA on Ser 311.

Both aPKC isoforms have been described as forming complexes with Par6 and Par3 (Noda et al., 2003; Henrique and Schweisguth, 2003; Joberty et al., 2000) to build a ternary complex (also called polarity complex (Suzuki and Ohno, 2006). Recent work has also identified nuclear accumulation of Par6 in MDCK cells after LMB treatment indicating nucleocytoplasmic shuttling similar to that we observed for aPKC (Cline and Nelson, 2007). Cline could not identify a specific nuclear function for Par6, but a participation in gene transcription, RNA splicing and mRNA transport was excluded.

Par3 has also been found to be located in the nucleus (Fang et al., 2007). In this case an association with Ku70/Ku80 proteins was reported and functional analysis revealed that Par3 regulates DNA-PK activity through this interaction which is needed in the repair of double-strand breaks. Neither Par6 nor Par3 has been evaluated for aPKC interaction/complex capability. Thus aPKC could be involved in individual nuclear functions with Par6 and/or Par3 but in addition it is also conceivable that the well established polarity complex (Par6/aPKC/Par3) exists in the nucleus independently and fulfills as yet uncharacterized functions.

It is necessary at this point to mention that the N-terminal constructs ($PKC\iota^{AA1\text{-}177}$ and $PKC\zeta^{AA1\text{-}176}$) we have used in our study have an average molecular weight of around 55 kDa (and even smaller with regard to the individual hinge constructs). Thus as a consequence we are not able to exclude that some of our immunfluoresence data are discolored by the fact that smaller proteins can enter the nucleus by passive diffusion (Nigg, 1997). Regardless of this fact we are convinced that our major findings are not influenced by this fact since all relevant mutation have been introduced and analysed in the full length proteins as well. In addition also the hinge domains have been tested in the context of a bigger fusion protein.

In conclusion, evidence for the implication of aPKCs in nuclear function(s) are accumulating, some may be redundant and some may be assigned to a single aPKC isoform. The functions may be dependent on specific stimuli since we have found that defined domains within the aPKC protein have various influences on the nuclear translocation behavior of the protein. Future challenges include the identification of the physiological conditions in which individual aPKC isoforms translocate to the nucleus which may then suggest links to specific nuclear function.

Materials and Methods

Cell cultures

Madin Darby Canine Kidney (MDCK) cells were grown in Gibco DMEM+GlutaMAX™-I (Invitrogen) with 15% Gibco fetal calf serum (Invitrogen), Gibco non essential amino acids (Invitrogen), Penicillin (50 units/ml) and streptomycin (100 µg/ml) (Invitrogen). For the nuclear export experiments, Leptomycin B (Sigma-Aldrich) was added to the medium to a final concentration of 4 ng/ml.

Plasmid constructions and site-directed mutagenesis

The murine cDNA was amplified from mouse brain RNA after reverse transcription by PCR using HotStarTaq Master Mix from QIAGEN (203,443). Following Primers were used: ι/λPKCwt for: CAC CAT GCC GAC CCA GAG GGA CAG CAG C; ι/λPKCwt rev: GAC ACA CTC TTC TGC AGA CAT CAA GAG GGG; ζPKCwt for: CAC CAT GCC CAG CAG GAC GGA CCC CAA GAT G; ζPKCwt rev: CAC GGA CTC CAC AGC AGA CAG CAG AA; ι/λPKCΔC rev: ACT GGA CGA CGC TTT ACC ACT CTC CCT GG; ζPKCΔC: CCC CTG AGA GAT TTT GAT CCC ATC CAC; ι/λPKC AA1-186rev: GAC CAG CTT GTG GCA CTT CTT ATG; ζPKC AA1-178rev: GAC GAG GAC GTG GCA GCG TTT ATG GAC; ι/λPKC AA27-247 for CAC CAT GTC CCA CAC GGT CGC GTG; ζPKC AA18-246: CAC CATGCG CGT CCG TCT GAA GGC GCA CTA CGG; ι/λPKC Hinge for: CAC CATGAC AAT TGA GTG TGG GCG GCA CT; ζPKC Hinge: CAC CATGGC TGA CCT GCA GGA GGC ATA TGG AT. All PCR products were sub-cloned into pENTR-D-TOPO by using the Gateway cloning system (Invitrogen) according to the manufacturer's instructions. All plasmids were verified by restriction enzymes and sequencing to confirm the correct coding sequence. All expression plasmids were constructed using the LR clonase Kit (Invitrogen) according to the manufacturer's instructions. The pDEST expression vector with a c-terminal GFP-tag was provided by Kjetil Tasken (The Biotechnology Centre of Oslo, Norway). For sequencing of the constructs we used following primer EGFP-N rev: CTGAACTTGTGGCCGTTTAC EGFP-N for: TCCGCCCCATTGACGCAA. For the site directed mutagenesis we used the Quickchange Site Directed Mutagenesis Kit (NO. 200518, Stratagene). The primer-design was done with the Quick Change Primer Design tool on the companies homepage. Following primers were used for the mutagenesis: ι/λPKCR141/142E for: GCC AAA CGT TTC AAT GAG GAG GCC CAC TGT GCC ATC; ι/λPKCR141/142E rev: GAT GGC ACA GTG GGC GCG CCT ATT GAA ACG TTT GGC; ι/λPKCR142G for: GCC AAA CGT TTC AAT AGG GGC GCC CAC TGT GC; ι/λPKCR142G rev: GCA CAG TGG GCG CCC CTA TTG AAA CGT TTG GC;

ζPKCR140/141E for: AAG CCA AGC GCT TTA ACG AGG AAG CGT ACT GCG GCC AG; ζPKCR140/141E rev: CTG GCC GCA GTA CGC TTC CTC GTT AAA GCG CTT GGC TT; ζPKCG141R for: AGC GCT TTA ACA GGA GAG CGT ACT GCG GC; ζPKCG141R rev: GCC GCA GTA CGC TCT CCT GTT AAA GCG CT; ι/λPKCD63A for: CAC CAT GAA ATG GAT AGC TGA GGA AGG AGA CCC AT; ι/λPKCD63A rev: ATG GGT CTC CTT CCT CAG CTA TCC ATT TCA TGG TG; ζPKCD62A for: CCT CAA GTG GGT GGC CAG TGA AGG TGA CC; ζPKCD62A rev: GGT CAC CTT CAC TGG CCA CCC ACT TGA GG.

To generate aPKCζN-ιHINGE and aPKCιN-ζHinge constructs we designed primers to add an additional BfaI restriction site to the N-terminus of the corresponding Hinge-region and the C-terminus of the N-terminal region without changing the amino acid sequence. The following primers were used: ι/λPKCN-Bfarev: GAC TAG GAC GTG GCA CTT CTT ATG; ι/λPKCHINGE-Bfafor:

GTC CTA GTC ACA ATT GAG TGT GGG CGG CAC T; ζPKCN-Bfarev: GAC TAG GAC GTG GCA GCG TTT ATG GAC; ζPKCHINGE-Bfafor: GTC CTA GTC CCG CTG ACC TGC AGG AGG CAT ATG GAT.

Both PCR products were sub-cloned into the pCRII-Topo plasmid according to the manufactures protocol (Invitrogen). The fragments were then excised using BamHI/EcoRV for the Hinge fragments and HindIII/XbaI for the N-terminal fragments. Afterwards all fragments were digested with BfaI and ligation was performed using the T4 DNA ligase from NEB according to the manufacturers protocol. The ligation product was amplified using a specific primer set (see above) and sub-cloned into the pENTR vector according to the manufacturers protocol.

For the chimeric full length constructs (aPKCι$^{\text{-zeta HINGE}}$, aPKCζ$^{\text{-iHINGE}}$) a similar approach was chosen. An additional EcoRI site was added to the PCR products of the kinase domain and aPKCζN-ιHINGE and aPKCιN-ζHinge constructs using specially designed primers: ι/λkinaseEcoRIfor: GAA TTC CTA GGT CTG CAG GAT TTC G; ι/λPKCΔCEcoRIrev: GAA TTC ACT GGA CGA CGC TTT ACC ACT CTC CCT GG; ζkinase EcoRIfor: GAA TTC CTG GGG CTG CAA GAC TTC G; ζPKCΔCEcoRIrev: GAA TTC CCC CTG AGA GAT TTT GAT CCC ATC CAC.

The PCR products were then subcloned into pCRII-Topo plasmid. The resulting plasmid was digested with EcoRI for 16 h at 37℃ to create EcoRI fragments. Both fragments were ligated with T4 DNA ligase (NEB) according to the manufacturer's protocol. The ligation product was amplified by PCR using primers for the wild-type full-length sequence and the PCR product was further sub-cloned into the pENTR vector. All constructs were verified by Restriction pattern and sequencing.

Subcellular localization analyzes and immunocytochemistry

For the sub-cellular localization studies of the different GFP fusion proteins, MDCK cells were seeded in a 4-well dish with a 14 mm microscope cover glass (Marienfeld), coated with 0.2% Gelantine at a density of 7.3×10^6 per well 18 h before transfection. The cells were then transfected with 0.8 µg of expression vector using Lipofectamine. The cells were fixed with 4% paraformaldehyde for 15 min and permeabilized in 0.01% Triton X-100 for 10 min at room temperature, 24 hours after transfection. We used the Vectashield mounting medium with DAPI (Vector) to mount the cells on a microscope slide (VWR). The GFP fusion proteins were visualized by confocal microscopy using the Zeiss LSM 510 Meta invert microscope equipped with a Zeiss LSM laser module and a AxioCam HMr digital camera.

Image analysis

The color digital images of the fluorescing cells were processed by the Adobe Photoshop CS5 (Adobe Systems Inc., USA) and analyzed by the ImageJ 1.43r (National Institute of Health, USA, http://rsb.info.nih.gov/ij) software. The 'Mean Gray Value' was quantitatively assessed in the selected regions of interest (ROI "Oval Selection") from the images using "Analyze" plugin ("Measure" option). The obtained data were in the arbitrary units of the 8-bit gray scale (0–256 units). Ratios were presented as means with standard deviations.

Data analysis

The histogram analysis of the fluorescence signal was performed with the profile tool provided by the LSM Image Examiner from Zeiss. The software enables the user to analyze the pixel strength of a defined area and all channels. We used the linear tool to analyze the localization of the GFP-fusion protein within the cell. To visualize and analyze the dimension of a cell and the position of the nucleus we used Alexa Fluor® 647 (Invitrogen) labeled Wheat Germ Agglutinin (WGA). In the histogram each peak represents a cell membrane. The two outer peaks represent the outer cell membrane and the inner peaks the nuclear envelope. The position and dimensions of the nucleus were visualized and analyzed by using 4′,6-diamidino-2-phenylindole (DAPI). Channel coding: red = WGA, blue = DAPI, green = GFP.

Western Blot analysis

MDCK cells were transfected according to the Lipofectamine 2000© transfection reagent from Invitrogen dependent of the size of the used cell culture dish. 24 hours after transfection the cells were trypsinized with 1 × Trypsin (Invitrogen) for 10 min at room temperature, the reaction was stopped by supplementing DMEM containing 15% FCS. The pellet was collected and incubated in 80 µl of protein extraction buffer (50 mM Tris/HCl, pH 7.5–8.0; 2 mM EDTA, pH 7.0; 10 mM EGTA, pH 7.0; 0.1% TritonX-100, 3% β-mercaptoethanol) supplemented with Proteinase Inhibitor Cocktail (Sigma, NO. P-2714), incubated on ice for 20 min. After supplementation of 25 µl of protein sample loading buffer the samples were boiled for 5 min. Subsequently. the samples were run on a 10% SDS-polyacrylamide gel and blotted onto BioRad nitrocellulose membranes. The membranes were blocked in 5% nonfat dry milk in TBST for 1 h at room temperature. Incubation with the primary antibody happened overnight in TBST at 4℃. The following antibodies were used: anti-GFP (Santa Cruz Antibodies NO. sc-8334) (1:500).

Acknowledgements

We are grateful to Jorunn Solheim for technical assistance and Catherine Jackson for incredible editorial work on the manuscript. Sebastian Seidl is a fellow of Molecular Life Science - University of Oslo.

Competing Interests

The authors would like to declare that they do not have conflicting financial interests.

References

Akimoto, K., Mizuno, K., Osada, S., Hirai, S., Tanuma, S., Suzuki, K. and Ohno, S. (1994). A new member of the third class in the protein kinase C family, PKC lambda, expressed dominantly in an undifferentiated mouse embryonal carcinoma cell line and also in many tissues and cells. *J. Biol. Chem.* **269**, 12677-12683.

Bandyopadhyay, G., Standaert, M. L., Sajan, M. P., Kanoh, Y., Miura, A., Braun, U., Kruse, F., Leitges, M. and Farese, R. V. (2004). Protein kinase C-lambda knockout in embryonic stem cells and adipocytes impairs insulin-stimulated glucose transport. *Mol. Endocrinol.* **18**, 373-383.

Bjørkøy, G., Lamark, T., Brech, A., Outzen, H., Perander, M., Øvervatn, A., Stenmark, H. and Johansen, T. (2005). p62/SQSTM1 forms protein aggregates degraded by autophagy and has a protective effect on huntingtin-induced cell death. *J. Cell Biol.* **171**, 603-614.

Clausen, T. H., Lamark, T., Isakson, P., Finley, K., Larsen, K. B., Brech, A., Øvervatn, A., Stenmark, H., Bjørkøy, G., Simonsen, A. et al. (2010). p62/SQSTM1 and ALFY interact to facilitate the formation of p62 bodies/ALIS and their degradation by autophagy. *Autophagy* **6**, 330-344.

Cline, E. G. and Nelson, W. J. (2007). Characterization of mammalian Par 6 as a dual-location protein. *Mol. Cell. Biol.* **27**, 4431-4443.

Díaz-Meco, M. T., Municio, M. M., Frutos, S., Sánchez, P., Lozano, J., Sanz, L. and Moscat, J. (1996). The product of par-4, a gene induced during apoptosis, interacts selectively with the atypical isoforms of protein kinase C. *Cell* **86**, 777-786.

Diaz-Meco, M. T. and Moscat, J. (2001). MEK5, a new target of the atypical protein kinase C isoforms in mitogenic signaling. *Mol. Cell. Biol.* **21**, 1218-1227.

Duran, A., Diaz-Meco, M. T. and Moscat, J. (2003). Essential role of RelA Ser311 phosphorylation by zetaPKC in NF-kappaB transcriptional activation. *EMBO J.* **22**, 3910-3918.

Durgan, J., Kaji, N., Jin, D. and Hall, A. (2011). Par6B and atypical PKC regulate mitotic spindle orientation during epithelial morphogenesis. *J. Biol. Chem.* **286**, 12461-12474.

Fang, L., Wang, Y., Du, D., Yang, G., Tak Kwok, T., Kai Kong, S., Chen, B., Chen, D. J. and Chen, Z. (2007). Cell polarity protein Par3 complexes with DNA-PK via Ku70 and regulates DNA double-strand break repair. *Cell Res.* **17**, 100-116.

Farese, R. V., Sajan, M. P., Yang, H., Li, P., Mastorides, S., Gower, W. R., Jr, Nimal, S., Choi, C. S., Kim, S., Shulman, G. I. et al. (2007). Muscle-specific knockout of PKC-lambda impairs glucose transport and induces metabolic and diabetic syndromes. *J. Clin. Invest.* **117**, 2289-2301.

Frutos, S., Moscat, J. and Diaz-Meco, M. T. (1999). Cleavage of zetaPKC but not lambda/iotaPKC by caspase-3 during UV-induced apoptosis. *J. Biol. Chem.* **274**, 10765-10770.

Galvez, A. S., Duran, A., Linares, J. F., Pathrose, P., Castilla, E. A., Abu-Baker, S., Leitges, M., Diaz-Meco, M. T. and Moscat, J. (2009). Protein kinase Czeta represses the interleukin-6 promoter and impairs tumorigenesis in vivo. *Mol. Cell. Biol.* **29**, 104-115.

Henrique, D. and Schweisguth, F. (2003). Cell polarity: the ups and downs of the Par6/aPKC complex. *Curr. Opin. Genet. Dev.* **13**, 341-350.

Hirano, Y., Yoshinaga, S., Ogura, K., Yokochi, M., Noda, Y., Sumimoto, H. and Inagaki, F. (2004). Solution structure of atypical protein kinase C PB1 domain and its mode of interaction with ZIP/p62 and MEK5. *J. Biol. Chem.* **279**, 31883-31890.

Hirano, Y., Yoshinaga, S., Takeya, R., Suzuki, N. N., Horiuchi, M., Kohjima, M., Sumimoto, H. and Inagaki, F. (2005). Structure of a cell polarity regulator, a complex between atypical PKC and Par6 PB1 domains. *J. Biol. Chem.* **280**, 9653-9661.

Horikoshi, Y., Suzuki, A., Yamanaka, T., Sasaki, K., Mizuno, K., Sawada, H., Yonemura, S. and Ohno, S. (2009). Interaction between PAR-3 and the aPKC-PAR-6 complex is indispensable for apical domain development of epithelial cells. *J. Cell Sci.* **122**, 1595-1606.

Huber, T. B., Hartleben, B., Winkelmann, K., Schneider, L., Becker, J. U., Leitges, M., Walz, G., Haller, H. and Schiffer, M. (2009). Loss of podocyte aPKClambda/iota causes polarity defects and nephrotic syndrome. *J. Am. Soc. Nephrol.* **20**, 798-806.

Joberty, G., Petersen, C., Gao, L. and Macara, I. G. (2000). The cell-polarity protein Par6 links Par3 and atypical protein kinase C to Cdc42. *Nat. Cell Biol.* **2**, 531-539.

Kovac, J., Oster, H. and Leitges, M. (2007). Expression of the atypical protein kinase C (aPKC) isoforms ι/λ and ζ during mouse embryogenesis. *Gene Expr. Patterns* **7**, 187-196.

Kudo, N., Wolff, B., Sekimoto, T., Schreiner, E. P., Yoneda, Y., Yanagida, M., Horinouchi, S. and Yoshida, M. (1998). Leptomycin B inhibition of signal-mediated nuclear export by direct binding to CRM1. *Exp. Cell Res.* **242**, 540-547.

Lamark, T., Perander, M., Outzen, H., Kristiansen, K., Øvervatn, A., Michaelsen, E., Bjørkøy, G. and Johansen, T. (2003). Interaction codes within the family of mammalian Phox and Bem1p domain-containing proteins. *J. Biol. Chem.* **278**, 34568-34581.

Lamark, T., Kirkin, V., Dikic, I. and Johansen, T. (2009). NBR1 and p62 as cargo receptors for selective autophagy of ubiquitinated targets. *Cell Cycle* **8**, 1986-1990.

Leitges, M., Sanz, L., Martin, P., Duran, A., Braun, U., García, J. F., Camacho, F., Diaz-Meco, M. T., Rennert, P. D. and Moscat, J. (2001). Targeted disruption of the zetaPKC gene results in the impairment of the NF-kappaB pathway. *Mol. Cell* **8**, 771-780

Lin, D., Edwards, A. S., Fawcett, J. P., Mbamalu, G., Scott, J. D. and Pawson, T. (2000). A mammalian PAR-3-PAR-6 complex implicated in Cdc42/Rac1 and aPKC signalling and cell polarity. *Nat. Cell Biol.* **2**, 540-547.

Lischka, P., Rosorius, O., Trommer, E. and Stamminger, T. (2001). A novel transferable nuclear export signal mediates CRM1-independent nucleocytoplasmic shuttling of the human cytomegalovirus transactivator protein pUL69. *EMBO J.* **20**, 7271-7283.

Martin, P., Duran, A., Minguet, S., Gaspar, M.-L., Díaz-Meco, M. T., Rennert, P., Leitges, M. and Moscat, J. (2002). Role of zeta PKC in B-cell signaling and function. *EMBO J.* **21**, 4049-4057.

Murray, N. R., Weems, J., Braun, U., Leitges, M. and Fields, A. P. (2009). Protein kinase C betaII and PKCiota/lambda: collaborating partners in colon cancer promotion and progression. *Cancer Res.* **69**, 656-662.

Nigg, E. A. (1997). Nucleocytoplasmic transport: signals, mechanisms and regulation. *Nature* **386**, 779-787.

Noda, Y., Kohjima, M., Izaki, T., Ota, K., Yoshinaga, S., Inagaki, F., Ito, T. and Sumimoto, H. (2003). Molecular recognition in dimerization between PB1 domains. *J. Biol. Chem.* **278**, 43516-43524.

Oster, H. and Leitges, M. (2006). Protein kinase C alpha but not PKCzeta suppresses intestinal tumor formation in ApcMin/+ mice. *Cancer Res.* **66**, 6955-6963.

Palmeri, D. and Malim, M. H. (1999). Importin beta can mediate the nuclear import of an arginine-rich nuclear localization signal in the absence of importin alpha. *Mol. Cell. Biol.* **19**, 1218-1225.

Pankiv, S., Lamark, T., Bruun, J.-A., Øvervatn, A., Bjørkøy, G. and Johansen, T. (2010). Nucleocytoplasmic shuttling of p62/SQSTM1 and its role in recruitment of nuclear polyubiquitinated proteins to promyelocytic leukemia bodies. *J. Biol. Chem.* **285**, 5941-5953.

Parker, P. J. and Murray-Rust, J. (2004). PKC at a glance. *J. Cell Sci.* **117**, 131-132.

Perander, M., Bjorkoy, G. and Johansen, T. (2001). Nuclear import and export signals enable rapid nucleocytoplasmic shuttling of the atypical protein kinase C lambda. *J. Biol. Chem.* **276**, 13015-13024.

Pu, Y., Peach, M. L., Garfield, S. H., Wincovitch, S., Marquez, V. E. and Blumberg, P. M. (2006). Effects on ligand interaction and membrane translocation of the positively charged arginine residues situated along the C1 domain binding cleft in the atypical protein kinase C isoforms. *J. Biol. Chem.* **281**, 33773-33788.

Puls, A., Schmidt, S., Grawe, F. and Stabel, S. (1997). Interaction of protein kinase C zeta with ZIP, a novel protein kinase C-binding protein *Proc. Natl. Acad. Sci. USA* **94**, 6191-6196.

Rosse, C., Linch, M., Kermorgant, S., Cameron, A. J. M., Boeckeler, K. and Parker, P. J. (2010). PKC and the control of localized signal dynamics. *Nat. Rev. Mol. Cell Biol.* **11**, 103-112.

Sánchez, P., De Carcer, G., Sandoval, I. V., Moscat, J. and Diaz-Meco, M. T. (1998). Localization of atypical protein kinase C isoforms into lysosome-targeted endosomes through interaction with p62. *Mol. Cell. Biol.* **18**, 3069-3080.

Soloff, R. S., Katayama, C., Lin, M. Y., Feramisco, J. R. and Hedrick, S. M. (2004). Targeted deletion of protein kinase C lambda reveals a distribution of functions between the two atypical protein kinase C isoforms. *J. Immunol.* **173**, 3250-3260.

Steinberg, S. F. (2008). Structural basis of protein kinase C isoform function. *Physiol. Rev.* **88**, 1341-1378.

Suzuki, A. and Ohno, S. (2006). The PAR-aPKC system: lessons in polarity. *J. Cell Sci.* **119**, 979-987.

Suzuki, A., Yamanaka, T., Hirose, T., Manabe, N., Mizuno, K., Shimizu, M., Akimoto, K., Izumi, Y., Ohnishi, T. and Ohno, S. (2001). Atypical protein kinase C is involved in the evolutionarily conserved par protein complex and plays a critical role in establishing epithelia-specific junctional structures. *J. Cell Biol.* **152**, 1183-1196.

Uberall, F., Hellbert, K., Kampfer, S., Maly, K., Villunger, A., Spitaler, M., Mwanjewe, J., Baier-Bitterlich, G., Baier, G. and Grunicke, H. H. (1999). Evidence that atypical protein kinase C-lambda and atypical protein kinase C-zeta participate in Ras-mediated reorganization of the F-actin cytoskeleton. *J. Cell Biol.* **144**, 413-425.

Wodarz, A., Ramrath, A., Grimm, A. and Knust, E. (2000). Drosophila atypical protein kinase C associates with Bazooka and controls polarity of epithelia and neuroblasts. *J. Cell Biol.* **150**, 1361-1374.

Wooten, M. W., Geetha, T., Babu, J. R., Seibenhener, M. L., Peng, J., Cox, N., Diaz-Meco, M. T. and Moscat, J. (2008). Essential role of sequestosome 1/p62 in regulating accumulation of Lys63-ubiquitinated proteins. *J. Biol. Chem.* **283**, 6783-6789.

Yang, J.-Q., Leitges, M., Duran, A., Diaz-Meco, M. T. and Moscat, J. (2009). Loss of PKC lambda/iota impairs Th2 establishment and allergic airway inflammation in vivo. *Proc. Natl. Acad. Sci. USA* **106**, 1099-1104.